

---

# Rethinking Attention Output Projection: Structured Hadamard Transforms for Efficient Transformers

---

Shubham Aggarwal

Shubham\_agg@alumni.iitm.ac.in

Lokendra Kumar

lokendra63@alumni.iitm.ac.in

## Abstract

The dense output projection in multi-head attention scales quadratically with model dimension, contributing significantly to parameter count, memory footprint, and inference cost. We propose replacing this projection with a fixed, parameter-free Walsh–Hadamard Transform followed by a lightweight learnable affine rescaling, eliminating approximately 25% of attention parameters per block while preserving global cross-head interaction through an orthogonal, norm-preserving transformation. Across different model sizes, we demonstrate that this structured substitution maintains comparable or slightly superior downstream task performance on standard benchmarks, while achieving up to 7% aggregate parameter reduction, 8.9% peak memory savings, and 6.6% throughput improvement at scale, with efficiency gains growing monotonically with model size, batch size, and sequence length. Interestingly, we observe that structured Hadamard-based models exhibit a steeper validation loss curve relative to training FLOPs compared to their dense counterparts, suggesting more favorable compute utilization during training.

## 1 Introduction

The Transformer architecture, introduced by Vaswani et al. [12], has become the cornerstone of modern sequence modeling. Its central innovation, the multi-head attention (MHA) mechanism, enables the model to simultaneously attend to information from multiple representation subspaces by projecting queries, keys, and values into several heads and recombining their outputs through a dense projection. This design endows Transformers with strong representational capacity and has catalyzed remarkable progress across natural language processing, computer vision, and multimodal learning.

Despite this success, the expressiveness of MHA comes at a considerable cost. The dense output projection responsible for mixing attention heads scales quadratically with the model dimension, contributing substantially to the overall parameter count and computational overhead. As models continue to grow in scale, it has become increasingly apparent that Transformers are often over-parameterized, and that not all of this capacity translates to proportional gains in performance. This observation has motivated a growing body of research aimed at reducing the parameter burden and computational cost of Transformers while preserving, or even improving, their accuracy.

In this work, we revisit a fundamental yet underexplored component of the attention mechanism: the dense  $c \times c$  projection used to combine the outputs of attention heads. While prior efforts have focused on reducing redundancy within attention heads or MLP blocks, the head-mixing projection itself has received comparatively little scrutiny. We challenge the assumption that a full dense projection is necessary for effective head combination, and propose replacing it with a learned Hadamard transformation. This structured alternative substantially reduces both parameter count and computational cost, while achieving performance comparable to the standard dense projection. A schematic comparison between the standard dense projection and the proposed Hadamard-based layer is illustrated in Figure 1.

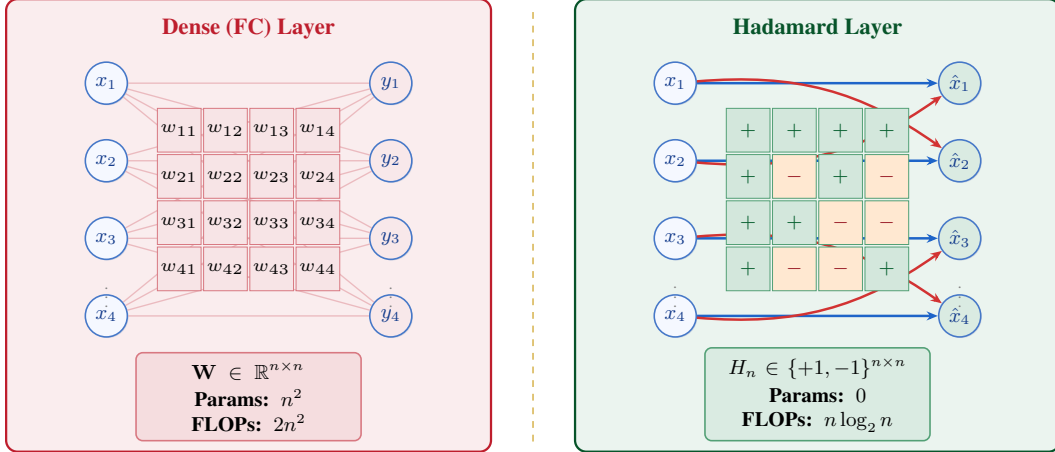


Figure 1: Comparative diagram of dense and Hadamard layers.

## 2 Related Work

**Parameter Efficiency in Attention Mechanisms.** Early efforts toward reducing attention cost focused on key-value sharing across heads. Shazeer [9] introduced *multi-query attention* (MQA), in which all heads share a single key-value projection, yielding substantial memory and latency reductions at the cost of modest quality degradation. Ainslie et al. [1] proposed *grouped-query attention* (GQA), which interpolates between MHA and MQA by partitioning query heads into groups sharing corresponding key-value heads, largely recovering full MHA accuracy while preserving inference efficiency. Together, these works establish that judicious parameter sharing across heads can yield meaningful efficiency gains, though overly aggressive sharing may compromise expressivity.

**Redundancy Across Attention Heads.** Cordonnier et al. [4] provided empirical evidence that a significant fraction of attention heads learn redundant key and query projections, motivating *collaborative multi-head attention*, which shares portions of key-query projections across heads with negligible accuracy loss. Jin et al. [6] approached head redundancy from a sparsity perspective via *mixture-of-heads* (MoH) attention, treating heads as experts and dynamically routing each token to a subset of heads, achieving competitive accuracy while activating only 50%–90% of available heads.

**Structured Parameterizations.** Wei et al. [14] demonstrated that low-rank and block-diagonal constraints on feedforward weight matrices can substantially reduce parameter counts with minimal accuracy degradation, establishing that structured matrix families are effective replacements for dense weights across Transformer components.

## 3 Motivation

Multi-head attention (MHA) derives its expressive power from attending to multiple representation subspaces in parallel. Given an input sequence, each attention head independently computes a weighted combination of values, producing a set of head-specific representations. These representations are concatenated and subsequently transformed by a dense linear projection, commonly referred to as the output projection. This projection plays a critical role: it enables interaction across heads, re-projects the concatenated representation back into the model dimension, and ensures compatibility with the residual connection that follows the attention block.

Despite its functional importance, the output projection constitutes a substantial fraction of the parameters within the attention module. As Transformer models scale, this dense transformation increasingly contributes to over-parameterization and computational cost. Empirical evidence from prior work suggests that attention heads exhibit a high degree of redundancy, and that full, unconstrained linear mixing across heads may not be strictly necessary to preserve model performance. This observation motivates the search for alternative head-mixing mechanisms that retain expressive capacity while reducing parameter count and computational overhead.

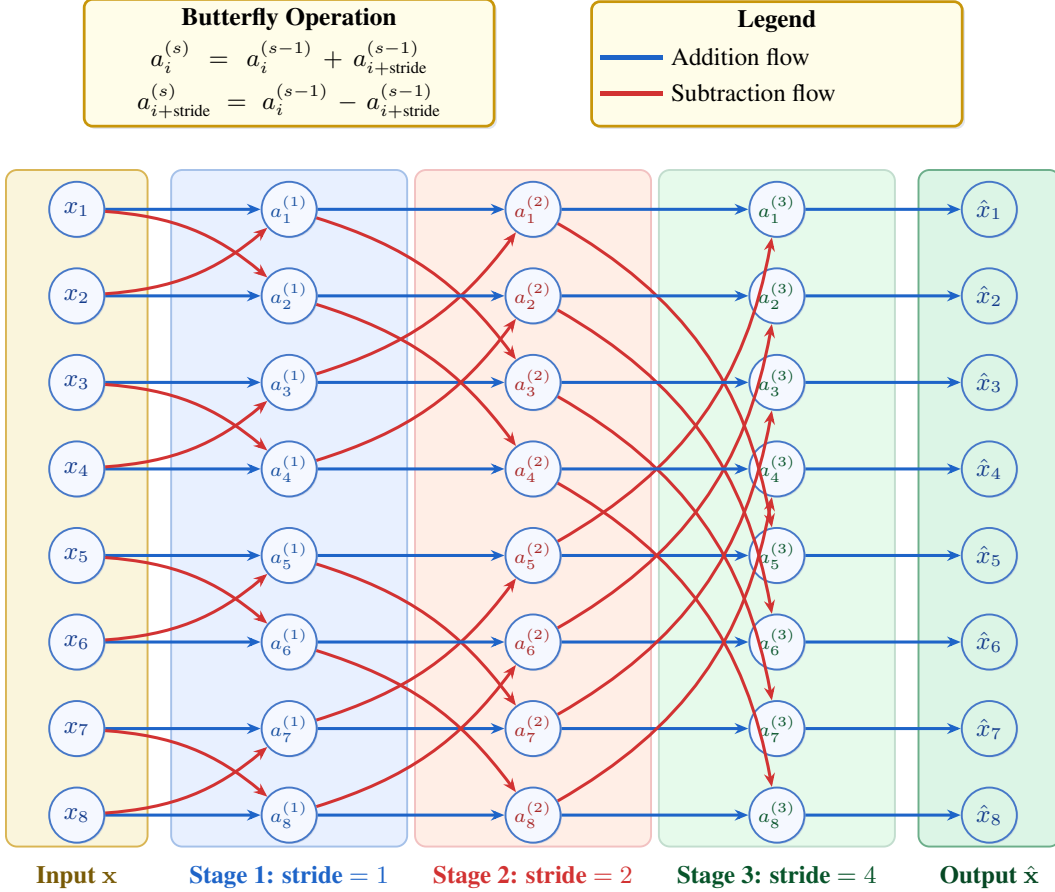


Figure 2: Computational flow of the Fast Walsh-Hadamard Transform (FWHT) showing the butterfly network structure with three stages

The Hadamard matrix presents a principled answer to this question. As a fixed, parameter-free orthogonal transform, the Walsh–Hadamard transform (WHT) uniformly mixes all input dimensions through a butterfly-structured computation (Figure 2), requiring no learned weights while preserving the  $\ell_2$  norm of its input. Crucially, this structured mixing is not merely a computational convenience—it imposes an inductive bias on how heads interact. Because the Hadamard transform couples every head output with every other through a fixed, maximally spread orthogonal basis, it encourages the model to distribute information across heads in a globally coherent manner. Rather than permitting arbitrary redundancy through unconstrained linear recombination, this structure implicitly regularizes the attention module: heads are incentivized to learn complementary, non-overlapping representations, since only such representations can be efficiently preserved and distinguished under a fixed orthogonal mixing. This is analogous in spirit to the role of orthogonal initialization in deep networks structured constraints that promote representational diversity without explicit supervision.

From a computational perspective, the WHT admits an  $\mathcal{O}(n \log n)$  butterfly factorization, replacing the  $\mathcal{O}(n^2)$  dense matrix multiply with a cascade of lightweight addition and subtraction operations across  $\log_2 n$  stages. Replacing the output projection with this transform eliminates a parameter matrix that typically accounts for roughly one-quarter of the total attention parameters in a standard MHA block, without introducing any new hyperparameters or architectural complexity.

Together, these properties—parameter efficiency, orthogonality, inductive bias toward complementary head representations, and computational regularity—motivate the use of the Hadamard transform as a structured drop-in replacement for the dense output projection in multi-head attention.

In this work, we propose to replace the dense output projection in attention block with a structured transformation based Hadamard matrix. By doing so, we preserve the essential role of head interaction

and dimensional consistency required for residual connections, while significantly reducing the number of learnable parameters. The resulting formulation removes a dense parameter matrix whose size scales quadratically with the model dimension, leading to a reduction of approximately one quarter of the total attention parameters in a standard multi-head attention block. In figure 2, we have shown the flow of the fast Walsh-Hadamard transform butterfly diagram, illustrating the three-stage computation for  $n=8$  inputs. This structured approach challenges the assumption that full dense mixing is necessary for effective head aggregation, suggesting that a fully dense projection may be unnecessarily overparameterized and offering a more parameter-efficient alternative.

## 4 Methodology

### 4.1 Architecture Overview

We propose a modified multi-head attention (MHA) block in which the dense output projection is replaced by a structured Hadamard-based mixing operation [5]. All other components—query, key, value projections, and per-head attention computation—remain unchanged.

Given input  $X \in \mathbb{R}^{T \times d_{\text{model}}}$ , standard MHA computes:

$$Q = XW_Q, \quad K = XW_K, \quad V = XW_V,$$

and produces concatenated head outputs  $Y = \text{Concat}(\text{Attn}_1, \dots, \text{Attn}_h) \in \mathbb{R}^{T \times d_{\text{model}}}$ , which are then mixed via a learned dense projection  $W_O \in \mathbb{R}^{d_{\text{model}} \times d_{\text{model}}}$ .

We replace this projection entirely with a fixed orthogonal Hadamard transform  $H \in \mathbb{R}^{d_{\text{model}} \times d_{\text{model}}}$ , satisfying  $H^\top H = d_{\text{model}}I$ , followed by a learnable affine rescaling:

$$\text{MHA}_{\text{Had}}(X) = \alpha \odot (YH) + \beta,$$

where  $\alpha, \beta \in \mathbb{R}^{d_{\text{model}}}$  are trainable scale and bias parameters. ( $H$  is orthogonal i.e  $1/n$ -embed)

The motivation is that full dense coupling across attention heads, while expressive, introduces quadratic parameter overhead and potential redundancy. The Hadamard transform achieves global, information-preserving cross-head interaction through additions and sign changes alone, substantially reducing parameter count while retaining sufficient expressive capacity through the affine parameters.

### 4.2 Parameter Efficiency Analysis

The attention block in standard MHA contains four dominant parameter matrices: query, key, value, and output projections, each contributing  $d_{\text{model}}^2$  parameters. Ignoring bias terms, the total number of attention parameters is therefore

$$4d_{\text{model}}^2,$$

with the output projection alone accounting for  $d_{\text{model}}^2$  parameters.

In the proposed formulation, the output projection matrix is removed entirely. The Hadamard matrix is fixed and parameter-free, while the affine rescaling introduces  $2d_{\text{model}}$  parameters. As a result, the total attention parameter count becomes

$$3d_{\text{model}}^2 + d_{\text{model}}.$$

( $3d_{\text{model}}^2$  parameters from K,Q,V and after ignoring bias  $d_{\text{model}}$  scaling parameters.)

The relative parameter reduction is thus

$$\frac{d_{\text{model}}^2 - d_{\text{model}}}{4d_{\text{model}}^2} \approx \frac{d_{\text{model}}^2}{4d_{\text{model}}^2} = \frac{1}{4},$$

corresponding to an approximate **25% reduction in attention parameters** per multi-head attention block.

### 4.3 Computational Complexity

For both standard MHA and the proposed method, the dominant computational cost arises from attention score computation:

$$\mathcal{O}(T^2 d_{\text{model}}),$$

Table 1: Comparison of dense and Hadamard (FWHT) linear layers.  $c$  denotes embedding dimension.

Property	Dense	Hadamard (FWHT)
Trainable parameters	$c^2$	0
Forward FLOPs	$\mathcal{O}(c^2)$	$\mathcal{O}(c \log c)$
Backward FLOPs	$\mathcal{O}(c^2)$	$\mathcal{O}(c \log c)$
Weight memory	$c^2$	0
Forward speedup	$1 \times$	$\frac{c}{\log_2 c} \times$
Numerical stability	depends on $W$	orthogonal
Expressivity	full-rank map	fixed orthogonal basis

which remains unchanged.

The difference lies in the *head-mixing* stage. Standard multi-head attention (MHA) performs head mixing using a dense matrix multiplication with computational complexity

$$\mathcal{O}(Td_{\text{model}}^2), \tag{1}$$

where  $T$  is the sequence length and  $d_{\text{model}}$  is the embedding dimension.

In contrast, the proposed method replaces this operation with a Fast Walsh–Hadamard Transform (FWHT) [8], yielding a complexity of

$$\mathcal{O}(Td_{\text{model}} \log d_{\text{model}}). \tag{2}$$

As illustrated in Figure 3, the forward FLOPs of dense matrix multiplication scale quadratically with the embedding dimension ( $c^2$ ), whereas the FWHT scales as  $c \log_2 c$ . The comparison is shown across embedding dimensions commonly used in GPT-2 models. Notably, FWHT introduces no additional trainable parameters, as it requires zero stored weights.

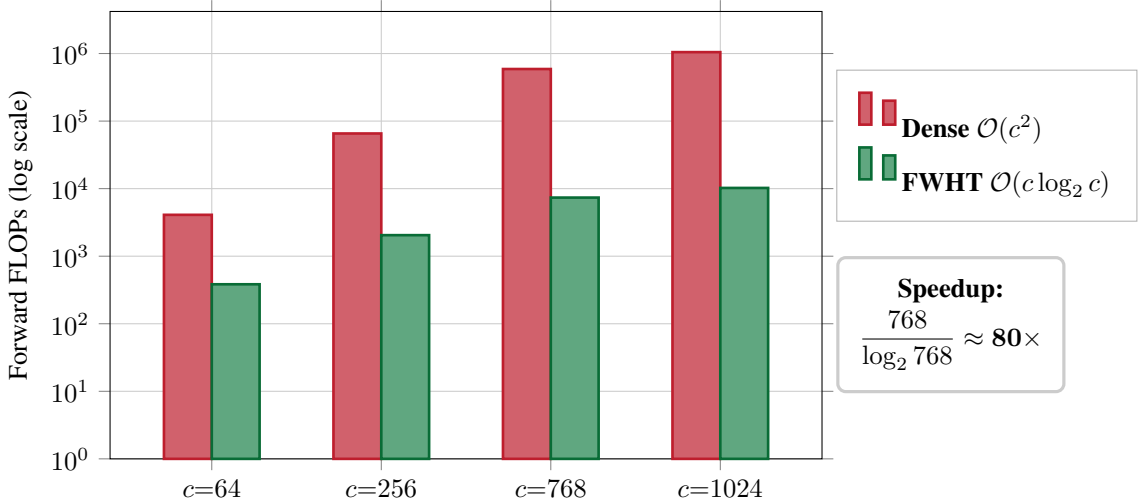


Figure 3: Forward FLOPs for dense matrix multiplication ( $c^2$ ) versus the Fast Walsh–Hadamard Transform ( $c \log_2 c$ ) across embedding dimensions used in GPT-2 (base:  $c=768$ ). FWHT requires zero stored weights.

## 5 Experiments

### 5.1 Experimental Setup

**Hardware and Implementation.** All experiments are conducted on  $8 \times$  NVIDIA H100 (80GB) GPUs under identical hardware conditions across all model variants to ensure fair comparison. All

Table 2: Sizes, architectures, and learning hyper-parameters of baseline models

Model Name	$n_{\text{params}}$	$n_{\text{layers}}$	$d_{\text{model}}$	$n_{\text{heads}}$	$d_{\text{head}}$	Batch Size	Learning Rate
Tiny	124M	12	768	12	64	0.25M	$6.0 \times 10^{-4}$
Small	354M	24	1024	16	64	0.25M	$3.0 \times 10^{-4}$
Base	757M	24	1536	16	96	0.50M	$2.5 \times 10^{-4}$

models are implemented in PyTorch, building upon the NanoGPT codebase [7] (with rope and swi glu) with modifications confined exclusively to the attention module. No additional architectural changes are introduced unless explicitly stated.

**Training Configuration** Training is performed in mixed-precision **bfloat16 (bf16)** using Distributed Data Parallel (DDP) across all 8 GPUs, with global batch sizes reported in tokens. All models are trained with a fixed context length of  $n_{\text{ctx}}=1024$ . We use the AdamW optimizer with  $b1=0.9$ ,  $b2=0.95$ ,  $e=10^{-8}$ , weight decay of 0.1, and gradient clipping at 1. The learning rate follows a cosine decay schedule with linear warmup; per-model learning rates are reported in Table 2.

## 5.2 Models Compared

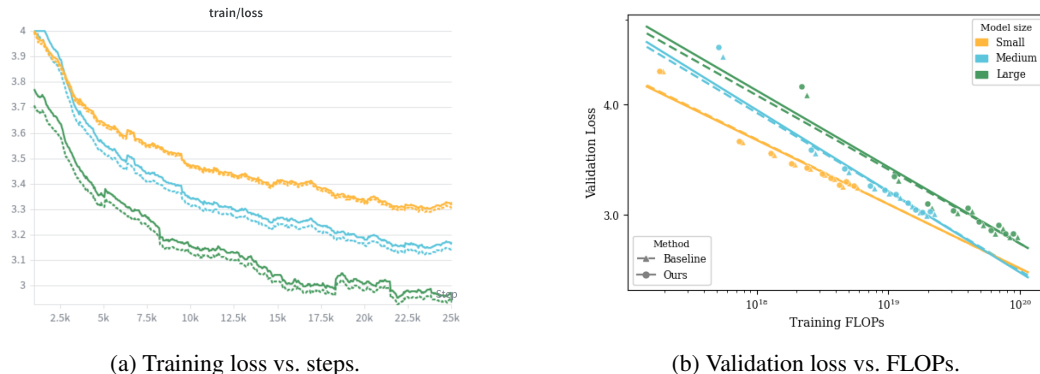


Figure 4: Comparison of three baseline models and three variants of our method across different sizes. Our models converge slightly slower (left) but show better scaling of validation loss with compute, with a steeper trend vs. FLOPs (right).

We evaluate the proposed attention mechanism by comparing it against baseline transformer derived from *NanoGPT* [7]. The baseline model follows a standard decoder-only Transformer architecture and incorporates *Rotary Positional Embeddings (RoPE)* [11] and *SwiGLU* [10] activation functions. This configuration serves as the reference implementation for all experiments.

**Baseline Models.** The baseline models use the original multi-head attention formulation with a standard output projection layer. We consider 3 baseline configurations corresponding to different model scales. In addition to the size of the model, all architectural components and training settings remain consistent across baseline variants.

**Proposed Models.** The proposed models are derived from the NanoGPT baseline by modifying only the attention module. Specifically, we replace the standard dense output projection in the multi-head attention block with the proposed Hadamard-based head mixing mechanism. All other architectural components are kept identical to the baseline. This controlled modification ensures that any observed differences in parameter count, computational cost, memory usage, or performance can be directly attributed to the proposed attention design.

### 5.3 Efficiency Results

We evaluate our method against the baseline along two primary axes: *inference efficiency*—throughput, latency, and peak memory—and *predictive performance* on downstream benchmarks. All efficiency experiments are conducted on a single NVIDIA H100-80GB GPU in BF16 precision unless otherwise stated.

#### 5.3.1 Prefill Phase

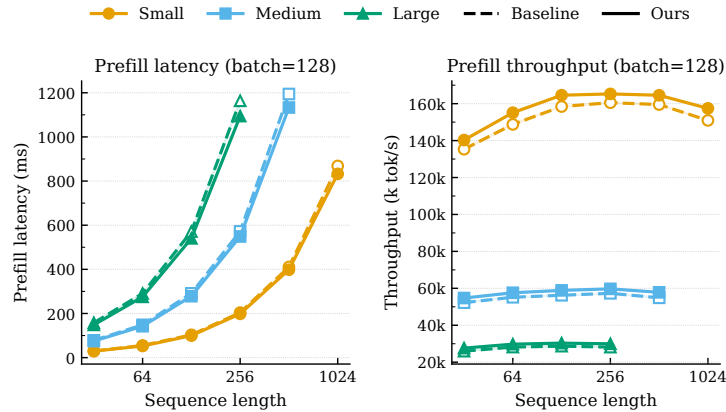


Figure 5: Prefill latency (ms) and throughput (tokens/s) as a function of sequence length at batch size 128. Our method consistently reduces latency and increases throughput across all model scales, with gains widening at longer sequences.

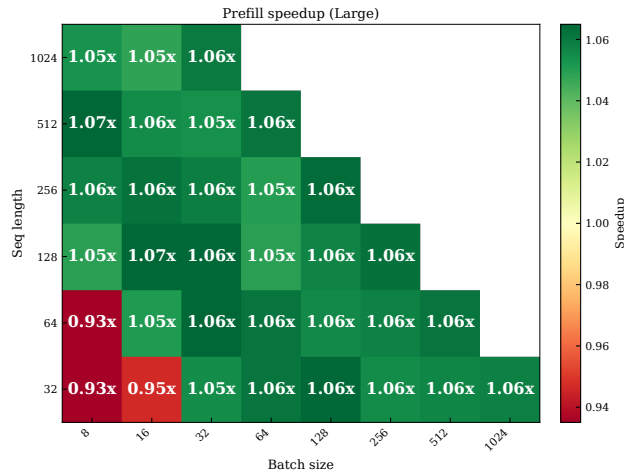


Figure 6: Prefill speedup heatmap across varying batch sizes and sequence lengths. Speedup grows monotonically with the product of batch size and sequence length, consistent with the increasing dominance of the memory-bandwidth-bound regime at larger token counts.

Figures 5 and 6 report prefill-phase results. Our method reduces latency and improves throughput across all evaluated model scales and sequence lengths. Speedup is most pronounced at large batch  $\times$  sequence length configurations, where the memory-bandwidth-bound regime dominates and structural parameter reduction yields the greatest benefit.

### 5.3.2 Decode Phase

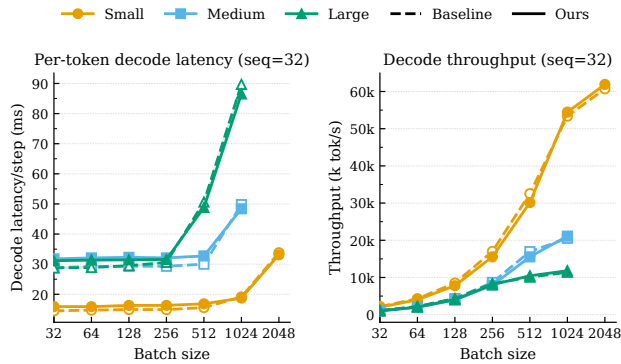


Figure 7: Decode throughput (tokens/s) and latency (ms) as a function of batch size at sequence length  $T=32$ . Our method scales more favorably with batch size, reflecting improved memory-bandwidth utilization in the single-token ( $T=1$ ) decode regime.

Figure 7 presents decode-phase results. Our method achieves consistent throughput improvements that grow with batch size, consistent with the memory-bandwidth-bound nature of autoregressive decoding.

### 5.3.3 Parameter Reduction

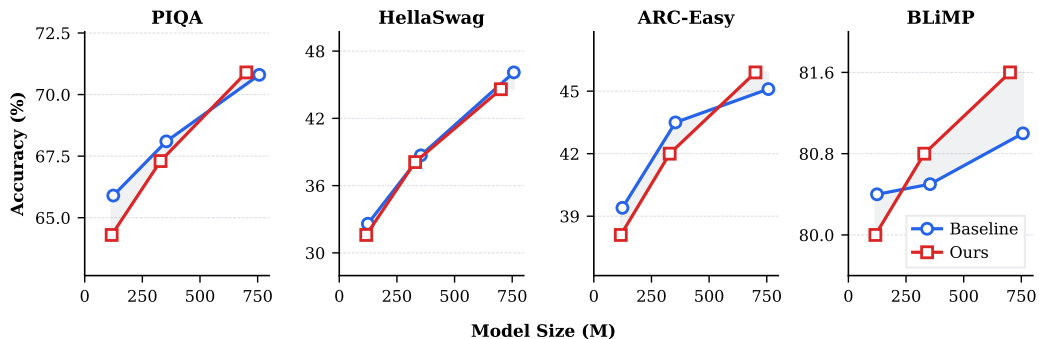
Replacing standard multi-head attention (MHA) with our proposed attention mechanism reduces total parameter count consistently across all three model scales (Small, Medium, and Large), yielding approximately 7% aggregate savings. Notably, the absolute reduction grows with model size, indicating that efficiency gains scale favorably as models increase in depth and width. These results align with the theoretical expectation of removing approximately 25% of attention parameters while leaving feedforward layers unchanged.

### 5.3.4 GPU Memory Usage

Table 3 summarizes peak GPU memory allocation alongside other decode-phase metrics. Our method reduces peak memory consumption consistently across all model sizes, directly enabling larger batch sizes within the same hardware budget—an important practical benefit for high-throughput serving workloads.

### 5.3.5 Downstream Evaluation

Our method achieves comparable accuracy to the baseline across several benchmarks, including PIQA [2], HellaSwag [15], ARC-Easy [3], and BLiMP [13], with marginal improvements on several tasks.



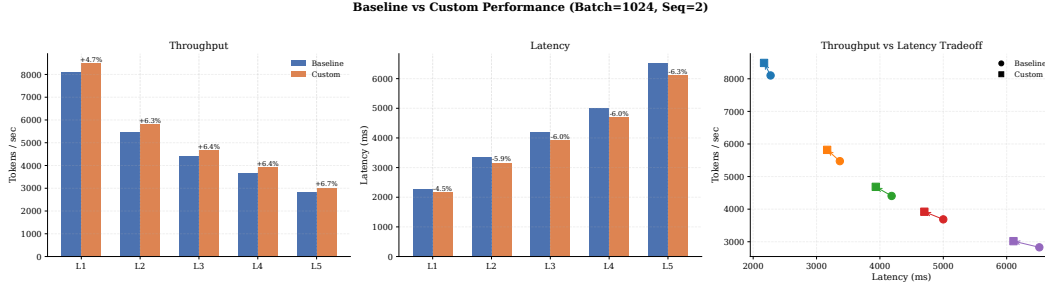


Figure 8: Decode throughput comparison (batch size 1024, sequence length 2) between the pretrained baseline and our method across all model sizes. Our method consistently outperforms the baseline, with gains increasing with model scale.

## 5.4 Scaling Studies

**Validity of Untrained Large-Scale Variants.** The Medium, Large, XL, and XXL configurations were not fully trained due to computational constraints. Crucially, decode-phase efficiency metrics—peak memory, latency, and throughput—are *independent of weight values*. Under the  $T=1$  decode setting, inference is memory-bandwidth bound: performance is governed by parameter count, tensor layout, KV cache footprint, and kernel execution characteristics, not by learned representations. Benchmarking with randomly initialized weights therefore yields valid and reproducible systems-level measurements, consistent with established practice in hardware-oriented decode profiling. The purpose of these larger configurations is to characterize the *scaling behavior of structural efficiency*, not model quality.

**Scaling Behavior.** Throughput gains increase monotonically with model size, from negligible improvement at Tiny scale to +6.6% at XXL (Table 3). The marginal regression at Tiny is expected: at small scale, kernel launch overhead and fixed runtime constants dominate execution time, masking the memory-bandwidth benefit. As model size grows, the proportion of time spent on memory transfers increases, and our structural reduction yields progressively greater benefit. The same trend holds along the batch and context-length axes: larger batches place more concurrent KV caches in HBM, and longer prompts produce larger per-sequence KV caches, both of which increase the relative share of memory traffic attributable to attention—the component our method directly optimizes.

Table 3: Decode-phase efficiency comparison across model sizes. All models evaluated at batch size 1024, sequence length 2 (decode step,  $T=1$ ), BF16 precision on a single H100-80GB GPU, following memory-bandwidth-bound decode benchmarking. ↓ lower is better; ↑ higher is better.  $\Delta$  denotes the relative change of our model vs. the baseline. Blue cells mark our model’s values; green  $\Delta$  = improvement, red  $\Delta$  = regression.

Size	Params			Peak Mem (MB) ↓			Latency (ms) ↓			Throughput (tok/s) ↑		
	Base	Ours	$\Delta$	Base	Ours	$\Delta$	Base	Ours	$\Delta$	Base	Ours	$\Delta$
Tiny	124M	<b>117M</b>	<b>-5.6%</b>	3490	<b>3454</b>	<b>-1.0%</b>	272	<b>275</b>	<b>+1.1%</b>	60 238	<b>59478</b>	<b>-1.3%</b>
Small	354M	<b>329M</b>	<b>-7.1%</b>	8620	<b>8525</b>	<b>-1.1%</b>	659	<b>635</b>	<b>-3.6%</b>	24 854	<b>25797</b>	<b>+3.8%</b>
Base	757M	<b>701M</b>	<b>-7.4%</b>	13 533	<b>13317</b>	<b>-1.6%</b>	1221	<b>1172</b>	<b>-4.0%</b>	13 417	<b>13974</b>	<b>+4.1%</b>
Medium	1.7B	<b>1.6B</b>	<b>-5.9%</b>	25 062	<b>24551</b>	<b>-2.0%</b>	2075	<b>1982</b>	<b>-4.5%</b>	7896	<b>8266</b>	<b>+4.7%</b>
Large	2.6B	<b>2.4B</b>	<b>-7.7%</b>	33 167	<b>32336</b>	<b>-2.5%</b>	3061	<b>2883</b>	<b>-5.8%</b>	5353	<b>5683</b>	<b>+6.2%</b>
XL	3.9B	<b>3.6B</b>	<b>-7.7%</b>	49 278	<b>48030</b>	<b>-2.5%</b>	4544	<b>4280</b>	<b>-5.8%</b>	3605	<b>3827</b>	<b>+6.2%</b>
XXL	5.6B	<b>5.1B</b>	<b>-8.9%</b>	62 312	<b>60584</b>	<b>-2.8%</b>	5920	<b>5551</b>	<b>-6.2%</b>	2767	<b>2951</b>	<b>+6.6%</b>
<b>Avg. <math>\Delta</math></b>	—	—	<b>-7.4%</b>	—	—	<b>-2.0%</b>	—	—	<b>-4.3%</b>	—	—	<b>+4.6%</b>

Naïvely reducing the embedding dimension  $n_{\text{embed}}$  or FFN expansion ratio produces irregular matrix sizes that misalign with Tensor Core–optimized dimensions (e.g., multiples of 64/128/256), degrading hardware utilization and potentially *increasing* latency despite fewer parameters. Our method reduces attention parameters while preserving GPU-aligned tensor shapes throughout, ensuring that hardware utilization does not regress. hence we didnt compare our models with vanilla variants

## 6 Limitations and Discussion

While the proposed Hadamard-based head-mixing layer reduces the theoretical number of operations, there remains significant scope for optimization in its practical implementation. In particular, highly optimized GEMM kernels benefit from decades of engineering effort, whereas our current Hadamard transform and scaling implementation is relatively naive. As a result, despite the reduced arithmetic complexity in theory, our experiments exhibit slightly longer training times compared to the theoretical gain it should have got. We expect that with optimized kernels and better hardware-aware implementations, the practical efficiency of the proposed approach can more closely match its theoretical advantages.

## 7 Conclusion

We have proposed an alternative head-mixing mechanism for multi-head attention that replaces the standard dense  $c \times c$  projection with a fixed Hadamard-based layer. While this modification affects only a single layer, its impact on parameter count, memory usage, and computational cost grows with model width and scale. As models become larger, the cumulative savings become increasingly significant, enabling more efficient inference and facilitating the deployment of attention-based models in performance- and memory-constrained settings.

## Acknowledgments

We thank Merai Private Limited for providing GPU resources used in our experiments.

## References

- [1] Joshua Ainslie, Sharan Wang, Aakanksha Bansal, Ankit Ramasamy, Jay Rao, and Illia Polosukhin. Gqa: Training generalized multi-query transformer models from multi-head checkpoints. *arXiv preprint arXiv:2305.13245*, 2023.
- [2] Yonatan Bisk, Rowan Zellers, Ronan Le Bras, Jianfeng Gao, and Yejin Choi. Piqa: Reasoning about physical commonsense in natural language, 2019.
- [3] Peter Clark, Isaac Cowhey, Oren Etzioni, Tushar Khot, Ashish Sabharwal, Carissa Schoenick, and Oyvind Tafjord. Think you have solved question answering? try arc, the ai2 reasoning challenge, 2018.
- [4] Jean-Baptiste Cordonnier, Andreas Loukas, and Martin Jaggi. Multi-head attention: Collaborate instead of concatenate. *arXiv preprint arXiv:2006.16362*, 2020.
- [5] Dao-AILab Contributors. Fast hadamard transform. <https://github.com/Dao-AILab/fast-hadamard-transform>, 2022. GitHub repository.
- [6] Peng Jin, Zhen Zhang, Hongyu Zhao, Yifan Zhou, and Jun Zhu. Moh: Multi-head attention as mixture-of-head attention. *arXiv preprint arXiv:2410.11842*, 2024.
- [7] Andrej Karpathy. nanogpt: The simplest, fastest repository for training/finetuning medium-sized gpts. <https://github.com/karpathy/nanoGPT>, 2022. GitHub repository. MIT License.
- [8] Quoc Viet Le, Tamas Sarlos, and Alexander Johannes Smola. Fastfood: Approximate kernel expansions in loglinear time, 2014.
- [9] Noam Shazeer. Fast transformer decoding: One write-head is all you need. *arXiv preprint arXiv:1911.02150*, 2019.
- [10] Noam Shazeer. Glu variants improve transformer, 2020.
- [11] Jianlin Su, Yu Lu, Shengfeng Pan, Ahmed Murtadha, Bo Wen, and Yunfeng Liu. Roformer: Enhanced transformer with rotary position embedding, 2023.

- [12] Ashish Vaswani, Noam Shazeer, Niki Parmar, Jakob Uszkoreit, Llion Jones, Aidan N. Gomez, Lukasz Kaiser, and Illia Polosukhin. Attention is all you need, 2023.
- [13] Alex Warstadt, Alicia Parrish, Haokun Liu, Anhad Mohananey, Wei Peng, Sheng-Fu Wang, and Samuel R. Bowman. Blimp: The benchmark of linguistic minimal pairs for english, 2023.
- [14] Xiang Wei, Yifan Zhang, Zhen Li, and Dawn Song. Building on efficient foundations: Effective training of llms with structured feedforward layers. In *Advances in Neural Information Processing Systems (NeurIPS)*, volume 37, pages 4689–4717, 2024.
- [15] Rowan Zellers, Ari Holtzman, Yonatan Bisk, Ali Farhadi, and Yejin Choi. Hellaswag: Can a machine really finish your sentence?, 2019.

## 8 Appendix

Table 4: Evaluation performance (%) across commonsense reasoning, science QA, and linguistic benchmarks. Our models are highlighted in gray.

Model	PIQA	HellaSwag	OpenBookQA	ARC-Easy	BLiMP
Baseline (Small)	65.9	32.6	27.0	39.4	80.4
Ours (Small)	64.3	31.6	29.8	38.1	80.0
Baseline (Base)	68.1	38.7	30.0	43.5	80.5
Ours (Base)	67.3	38.1	28.8	42.0	80.8
Baseline (Large)	70.8	46.1	32.8	45.1	81.0
Ours (Large)	70.9	44.6	31.5	45.9	81.6